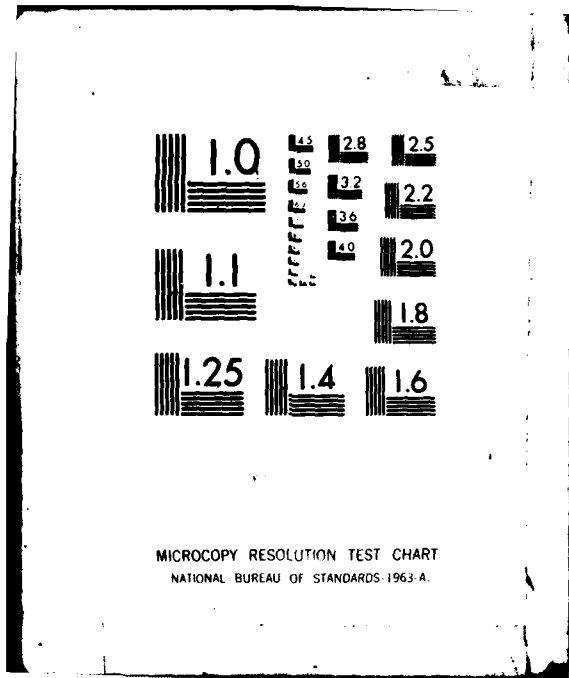


AD-A110 606 WASHINGTON UNIV SEATTLE DEPT OF CHEMISTRY F/8 7/4
VIBRATIONAL ENERGY TRANSFER AND PYROLYSIS OF NITROMETHANE BY TH--ETC(U)
JAN 82 W YUAN, B S RABINOVITCH, R TOSA N00014-75-C-0690
UNCLASSIFIED NL

1-4
4-5
5-6

END
DATE
FILED
3-12-82
DTIC



~~LEVEL~~

12

AD A110606

Vibrational Energy Transfer and Pyrolysis of Nitromethane
by the Variable Encounter Method

by W. Juan, B. S. Rabinovitch and R. Tosa

Department of Chemistry BG-10, University of Washington
Seattle, Washington 98195

Technical Report No. NR092-549-TR24

Contract N00014-75-C-0690, NR-092-549

January 15, 1982



Prepared for Publication in
Journal of Physical Chemistry

DTIC FILE COPY

OFFICE OF NAVAL RESEARCH
Department of the Navy
Code 473
800 N. Quincy
Arlington, VA 22217

Reproduction in whole or in part is permitted for any purpose of
the United States Government. This document has been approved for
public release; its distribution is unlimited.

Unclassified

SECURITY CLASSIFICATION OF THIS PAGE (When Data Entered)

DD FORM 1 JAN 73 1473 EDITION OF 1 NOV 68 IS OBSOLETE
S/N 0102 LF 014 6601

Unclassified

~~SECURITY CLASSIFICATION OF THIS PAGE (When Data Entered)~~

Vibrational Energy Transfer and Pyrolysis of Nitromethane by the Variable Encounter Method

by W. Yuan,[†] B. S. Rabinovitch and R. Tosa

Department of Chemistry BG-10, University of Washington
Seattle, Washington 98195

Abstract

The pyrolysis of nitromethane has been studied by the Variable Encounter Method (VEM) at temperatures from 816 K to 1092 K with two reactors of differing geometry having fused silica surfaces. The probability of reaction per collision with the reactor surface was measured. The down energy transition jump size, $\langle \Delta E' \rangle$, was determined. It decreased with increasing wall temperature. A comparison is made of $\langle \Delta E' \rangle$ with previous results reported to date for other substrate molecules. Nitromethane is one of the more efficient energy transfer agents. However, in addition to the size (vibrational eigenstate density) and the polarity of the molecules, the nature of the hot surface seems also to play a role.

Accession No. 1
NAME OF UNIT
LEVEL
UNITS
JULY 1968

By _____
Distribution
Available to states
List

A

Introduction

Nitromethane is a widely investigated species because of its importance in a number of phenomena including the mechanism of gas phase nitration of hydrocarbons, the mechanism of formation of photochemical smog, and the chemistry of propellants. A large amount of work¹⁻⁶ has been devoted to the study of the kinetics and mechanism of the thermal decomposition of nitromethane. However, virtually no attention has been paid to the study of vibrational energy transfer involving this species. Of course, collisional activation and deactivation is a fundamental physical process of great ubiquity. Since nitromethane is a highly polar compound, it is also of interest to study the behavior of this molecule by the VEM method which has been applied recently to a variety of molecules, principally non-polar hydrocarbons.^{7,8} By this technique, vibrational relaxation in the transient region may be studied, in principle, on a collision-by-collision basis.

In this method, a molecule equilibrated at some low temperature in a reservoir flask is allowed to enter a reactor of variable dimensions, say cylindrical, heated to reaction temperature (called an encounter). Two events are possible: the molecule may escape from the finger after a sequence of collisions with the hot wall; or the series of vibrational relaxation collisions with the wall may be terminated by a reaction event. Only subjects for which the decomposition reaction is a homogeneous process have been chosen for study. By varying the geometry of the finger, the average residence time of the molecule in the hot reaction zone can be varied; and the average number m of successive collisions that occur before the molecule exits from the finger (and re-equilibrates with the cold wall) can therefore be varied. The average reaction probability per encounter can be measured experimentally for different fingers, and a suitable

energy transfer model may be estimated by fitting the data. The collision events themselves may be simulated by a Monte Carlo calculation using the known reactor geometry; and a distribution function $f(n,m)$ may be found for the number of sequential collisions n that occur per encounter with a reactor of given m ($m = \bar{n}$).

In this paper we describe the study of nitromethane in two silica reactors at temperatures between 800 K and 1100 K.

Experimental

Nitromethane (Aldrich Chemical Company, 99%, spectrophotometric grade) was used without purification. Gas chromatographic analysis showed that it contained less than 0.5% nitroethane.

As was described previously,⁸ the apparatus consisted of a 1-liter fused quartz spherical reservoir flask which had two quartz cylindrical finger reactors blown on to the surface. These fingers were of cylindrical geometry having length/radius ratios of ~ 1.7 and ~ 6.4, corresponding to mean numbers of sequential collisions, $m = 5.0$ and 14.4, respectively. Each finger could be separately heated in a stainless steel furnace block which was maintained by ceramic clamshell Kanthal electric heaters. The temperature of each finger was measured with five chromel-alumel thermocouples cemented separately to the outside of the reactor finger. Typical reactor finger temperatures were ~ 800 K to ~ 1100 K; flask reservoir temperatures were 400 K to 480 K. The temperature variation during the run time was $\pm 1^{\circ}\text{C}$ and along the finger length was $\pm 10^{\circ}\text{C}$. The temperature of the reactor was estimated by simple averaging. The effective temperature of the cold flask was suitably weighted by surface area, but calculation showed that the effect on the theoretical calculation due to a change of the flask temperature by as much as 50°K was negligible. Before a run, the reactor and flask reservoir were evacuated to approximately $3 - 5 \times 10^{-6}$ torr. Reaction run pressures were in the range $7 - 8 \times 10^{-4}$ torr. Reaction time varied from several minutes to ten hours, depending on the reaction temperature. The reaction percentage varied between 2% to 40%. At the end of a run, the reaction mixture was expanded from the reactor into a liquid nitrogen trap.

Separation of the reaction products was made at 100°C on a 1-m column of 3-mm copper tubing packed with Porapak Q. The detector was FID. Acetonitrile, which is inert under these conditions,

was used as an internal standard against which the disappearance of substrate could be accurately measured. No attempt was made to monitor all of the product species, which for this system are very numerous.¹⁻⁵

Surface Seasoning

The surface condition of the hot finger had a significant influence on the observed rate constant. If the surface were seasoned with reactant itself as has been customary in all previous work — a technique that has led to minimal and reproducible rates of reaction — the rate constant became progressively higher although eventually leveling off. This suggested the possible presence of surface catalysis. It was found that oxidizing the surface at 1100 K with 30-40 torr pure oxygen for several hours and then evacuating the reactor to $3 - 5 \times 10^{-6}$ torr gave reproducible results and minimal rates of reaction. The oxidation procedure was carried out at each temperature studied.

Results and Discussion

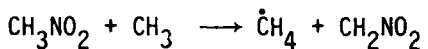
The thermal decomposition reaction obeys the first-order law. This is illustrated in Fig. 1. The apparent rate constants are summarized in Table I. Each tabulation is the average of from three to four determinations from separate runs. As Fig. 2 shows, the Arrhenius relation (which no longer has a simple meaning here) was satisfied for this temperature range. The apparent activation energies calculated from Fig. 2 are $38.8 \text{ kcal mole}^{-1}$, for the $m = 5$ finger, and $42.4 \text{ kcal mole}^{-1}$, for the $m = 14.4$ finger. The latter value, being closer to the low pressure steady state value, should, of course, be the higher one.

There exist several different experimental sets of high-pressure Arrhenius parameters for this reaction.¹⁻⁶ We chose to use the measurement of Glanzer and Troe,⁵ $E_a = 58.5 \text{ kcal mole}^{-1}$, which is quite close to the value calculated by Benson and O'Neal⁶ from thermodynamic quantities and mechanistic considerations. Since this activation energy is the highest of all those reported, we are inclined to believe that this choice is optimal. The GT and BO values for the frequency factor are peculiarly different, but these quantities have no bearing on our results; only E_a enters, i.e., the critical threshold E_0 , since our data were taken in the second-order region.

The vibrational spectrum of nitromethane has been assigned⁹ (see App. I). The value of E_0 for nitromethane was calculated to be $54.4 \text{ kcal mole}^{-1}$, with use of the average temperature 1150 K over the range used by GT and the activated complex model of App I.

The average probability of decomposition per collision with the hot wall in a reactor of given m -value, $\bar{P}_c(m)$, was calculated from the apparent first-order rate constants, the known reactor dimensions and the reservoir flask temperature. Since our rates were calculated from nitromethane disappearance, it is necessary to consider the possible extent of chain or sensitized character

of nitromethane pyrolysis. According to Perche's¹⁰ simplified mechanism used for computer simulation kinetics, the important secondary radical reactions which cause significant decomposition of nitromethane are



and



From the detailed product construction given by these authors at 700 K, the additional decomposition fraction of the parent is estimated at approximately 30%. Since these free radical reactions have low critical thresholds, the temperature increase in our system to the range 800 K-1000 K favors the unimolecular decomposition relative to these abstraction processes. Moreover, in our system the total pressure is very much lower than in the usual pyrolytic conditions so that it is expected that the importance of second order reactions are even further reduced. In fact, our rate constants were unaltered within experimental error when the reaction pressure was increased from 3×10^{-4} torr to 3×10^{-3} torr. This implies that in our system the observed rate constant is virtually independent of the role played by bimolecular secondary reactions and we have adopted the observed rate values as the correct ones. The $\bar{P}_c(m)$ values are collected in Table II and Fig. 3 for $m = 5$ and 14.4.

The computer simulation of the encounter activation process has been described elsewhere.^{7,15} Two models have been used to characterize the probability, p_{ij} of a down energy transition, ΔE , by the molecule from energy E_j to energy E_i :

Model FG (flat gaussian, i.e., ΔE_{mp} independent of E_j),

$$p_{ij} = A_1 \exp(-(\Delta E - \Delta E_{mp})^2/2\sigma^2) ;$$

Model BE (exponentially weighted Boltzmann),

$$p_{ij} = A_2 N(E_i) \exp(E_i/RT) \exp(-\Delta E/\langle \Delta E \rangle) .$$

The correlation table used in the computer simulation is given in Table III. The correlation coefficient C_j is defined as the probability that molecules which have already experienced j collisions with the hot wall will have at least the $(j+1)$ th collision, i.e., $C_j = \sum_{i=j+1}^{\infty} n_i / \sum_{i=j}^{\infty} n_i$, where n_i is the sum of the molecules in the distribution vector left after i collisions. The correlation coefficients summarize the varying probability of a molecule remaining in the reactor after each wall collision. The parameters of each particular model distribution were adjusted to provide theoretical agreement with the experimental curve for the $m = 5$ finger; the parameters so chosen were then used to calculate a theoretical curve for the $m = 14.4$ finger. Fit is made to the $m = 5$ curve because it provides greater sensitivity to model detail than does the $m = 14.4$ curve which lies closer to the steady state value. The graphs are shown in Fig. 3. It can be seen that the theoretical curves are close to the experimental value for $m = 14.4$, showing good concordance between the two sets of experimental data. The BE model fits the data somewhat better than the FG model but there is little to choose between them. A set of parameters for the FG model that exactly fit the experimental $m = 14.4$ data may be calculated and give somewhat higher values of $\langle \Delta E' \rangle$. Calculated steady state curves ($m = \infty$) as well as the strong collider curve are also given in Fig. 3, and it appears that the hot wall will approach the strong collider behavior when the temperature falls substantially below 800 K. Once again, the trend observed in previous VEM studies¹¹⁻¹³ of increasing strength of collisions with decreasing temperature is borne out. (However, the lowest temperature value for $m = 14.4$ appears somewhat too high.) The effective average energy of down transitions, $\langle \Delta E' \rangle$ for models BE and FG together with their parameters are summarized in Table IV.

Comparison with the previous results by the VEM method is made in Table V. A rough rule that the down jump energy transfer coefficient per collision of the substrate, declines with increasing size (i.e., increasing vibrational eigenstate density) of the molecule seemed evident from earlier studies with various hydrocarbon reactants.⁸ Also, it was shown that the polar molecule, iodopropane ($\mu = 2.0$ D), seems more efficient in energy transfer than non-polar ones, due to the longer sticking time that gives rise to more complete accommodation. The measured efficiency for highly polar nitromethane ($\mu = 3.6$ D), while one of the more efficient in Table IV, seems a little lower than expected (which, incidentally, also belies any significant role for surface catalysis). However, we note that in the present work an oxidized surface was used instead of the surface seasoned by the reactant itself, as in our previous studies, so that we may be seeing an effect of different energy transfer efficiency of the surface. Indeed, as mentioned above under Experimental, the rate (not reported) on a seasoned surface was larger; calculated values of the energy transfer on such a surface were found and gave magnitudes that even exceed those for iodopropane.

Clearly, apart from the polarity or size of molecules, the nature of the surface must play a significant role in molecule-surface relaxation process. We will attempt to clarify this feature in future studies.

Acknowledgment

We thank the Office of Naval Research for their support of this work.

Table I. Apparent Rate Constants for Decomposition

<u>m</u>	<u>T(K)</u>	<u>$10^6 k \text{ (sec}^{-1}\text{)}$</u>	
5.0	870	4.1	
		5.1	
		4.2	
		Av. 4.5 ± 0.6^a	
	987	59	
		70	
		64	
		84	
	1069	290	
		290	
		320	
		320	
14.4	816	12.5	
		10.1	
		8.4	
		12.2	
	907	139	
		143	
		176	
		133	
	1013	2000	
		1760	
		1780	
		1470	
	1092	8200	
		8000	
		7800	
Av. 1750 ± 100			
Av. 8000 ± 200			

a) Standard deviation of the mean

Table II. Experimental values of $10^8 \bar{P}_c(m)$

<u>m</u>	<u>T(K)</u>	<u>$10^8 \bar{P}_c(m)$</u>
5.0	870	1.3
	987	20
	1069	87
14.4	816	1.2
	907	16
	1013	180
	1092	800

Table III. Correlation Coefficients C_n

<u>n/m</u>	<u>5</u>	<u>14.4</u>
1	0.750	0.759
2	0.788	0.833
3	0.800	0.889
4	0.809	0.907
5	0.815	0.921
6	0.819	0.930
7	0.822	0.937
8	0.824	0.942
9	0.824	0.946
10	1	0.950
11	1	0.952
12		0.954
13		0.956
14		0.957
15		0.958
16		0.958
17		1
18		1

Table IV. Energy Transfer Parameters for Nitromethane

	<u>T(K)</u>	<u>816</u>	<u>907</u>	<u>1013</u>	<u>1092</u>
FG	$\langle \Delta E_{mp} \rangle$	2440	1960	1760	1700
	$\langle \Delta E' \rangle$	2700	2170	1950	1880
BE	$\langle \Delta E \rangle$	911	943	981	1090
	$\langle \Delta E' \rangle_{E_0}^a$	4970	4100	3360	3355

a) Energy level dependent value; given here at $E = E_0$

Table V. Comparison of $\langle \Delta E' \rangle$ (cm^{-1}) for Different Molecules

Molecule	E_0 / (kcal mole $^{-1}$)	n_t^a	Model	$\langle \Delta E' \rangle$ (cm^{-1})			Ref.
				800 K	900 K	1000 K	
Nitromethane	54.4	15	6	2840	2200	1960	1880
1-Iodopropane	48.5	27	6	3015			11
Cyclopropane	64	21	6	3050	2400	2100	2000
				3200	2500	2170	2040
Cyclopropane-d ₆	65.5	21	6	2300	2040	1890	1860
Cyclobutene	33	24	6	2010			15
Cyclobutane	63	30	Exp ^c	2180	1800	1600	1480
				6	2700	2125	1925
Methylcyclopropane	61	30	Exp	1860	1550	1440	1415
							17

a) The number of internal degrees of freedom

b) Some values obtained by interpolation or extrapolation

c) Flat exponential model

Appendix

Vibrational frequencies and parameters for RRKM calculations (cm⁻¹)

Nitromethane molecule:

3048(2), 2965, 1582, 1488, 1449, 1413, 1384, 1153, 1097, 921, 647, 599,
476, internal rotation ($\sigma = 6$).

Activated complex:

3048(2), 2965, 1582, 1488, 1449, 1413, 1384, 647, 200(2), 120(2), internal
rotation ($\sigma = 6$).

$$E_0 = 54.4 \text{ kcal mole}^{-1}$$

$$F = 1.3$$

References

[†] Visiting Scholar; permanent address: Department of Chemistry and Chemical Engineering, Qinghua University, Beijing, China.

1. Dubikhin, V. V.; Nazin, G. M.; Manelis, G. B. Akademija Nauk SSSR, Chemical Science Div. Bull. 1971, 1247.
2. Crawforth, C. G.; Waddington, D. J. J. Phys. Chem. 1970, 74, 2793; Trans. Faraday Soc. 1969, 65, 1334.
3. Nazin, G. M.; Manelis, G. B.; Dubovitskii, F. I. Russian Chemical Reviews 1963, 37, 603.
4. Zaslonko, I. S.; Kogarko, S. M.; Mozhukhin, E. B.; Petrov, Yu. P. Kinetics and Catalysis 1972, 13, 1001
5. Glanzer, K.; Troe, J. Helv. Chim. Acta 1972, 55, 2884; Troe, J. J. Chem. Phys. 1977, 66, 4758.
6. Benson, S. W.; O'Neal, H. E. "Kinetic Data on Gas Phase Unimolecular Reactions" NSRDS, Nat. Bur. Stds. #21, 1970, p. 473.
7. Kelley, D. F.; Zalotai, L.; Rabinovitch, B. S. Chem. Phys. 1980, 46, 379.
8. Yuan, W.; Tosa, R.; Chao, K.-J.; Rabinovitch, B. S. Chem. Phys. Lett. in press.
9. Wells, A. J.; Wilson, Jr., E. B. J. Chem. Phys. 1941, 9, 314.
10. Perche, A.; Tricot, J. C.; Lucquin, M. J. Chem. Research(S) 1979, 116, 1979, 304; 1979, 306.
11. Wolters, F. C.; Chao, K.-J.; Rabinovitch, B. S. Int. J. Chem. Kin. 1982, in press.
12. Kasai, T.; Kelley, D. F.; Rabinovitch, B. S. Chem. Phys. Lett. 1981, 81, 126.
13. Arakawa, R.; Kelley, D. F.; Rabinovitch, B. S. J. Chem. Phys. 1981,
14. Flowers, M. C.; Wolters, F. C.; Kelley, D. F.; Rabinovitch, B. S. J. Phys. Chem. 1981, 85, 849.
15. Wolters, F. C.; Flowers, M. C.; Rabinovitch, B. S. J. Phys. Chem. 1981, 85, 589.
16. Flowers, M. C.; Wolters, F. C.; Barton, B. D.; Rabinovitch, B. S. Chem. Phys. 1980, 47, 189.
17. Kelley, D. F.; Kasai, T.; Rabinovitch, B. S. J. Chem. Phys. 1980, 73, 5611.

Figure Captions

Fig. 1 First order law plots of $\ln(a-x)$ versus ct (sec)

\square , $T = 870$ K, $c = 10^{-5}$; $\triangle = T = 1068$ K, $c = 10^{-2}$

Fig. 2 Arrhenius plots of $\log_{10} k$ vs $1/T$ for the $m = 5.0$ and $m = 14.4$ reactors.

Fig. 3 Plots of $\bar{P}_c(m)$ versus $T(K)$ for the $m = 5.0$ and $m = 14.4$ reactors.

\blacksquare are the experimental points for the $m = 5.0$ reactor;

\square are the experimental points for the $m = 14.4$ reactor;

— and -·-·- are theoretical plots of BE model and FG model, fitted at $m = 5.0$, for the $m = 14.4$ reactor. The theoretical curve for the strong collider (SC) and for the $m = \infty$, steady-state case, calculated with the $m = 5.0$ parameters of the BE model, are also shown.

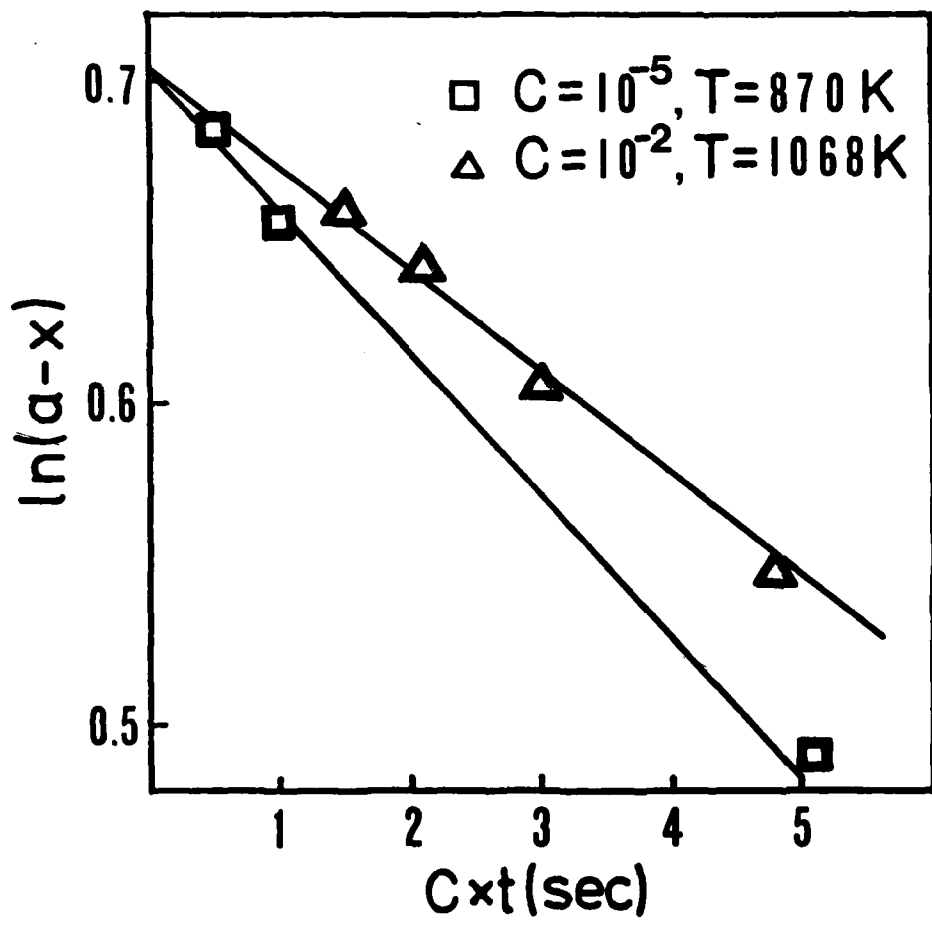


Fig. 1. Yuan et al.

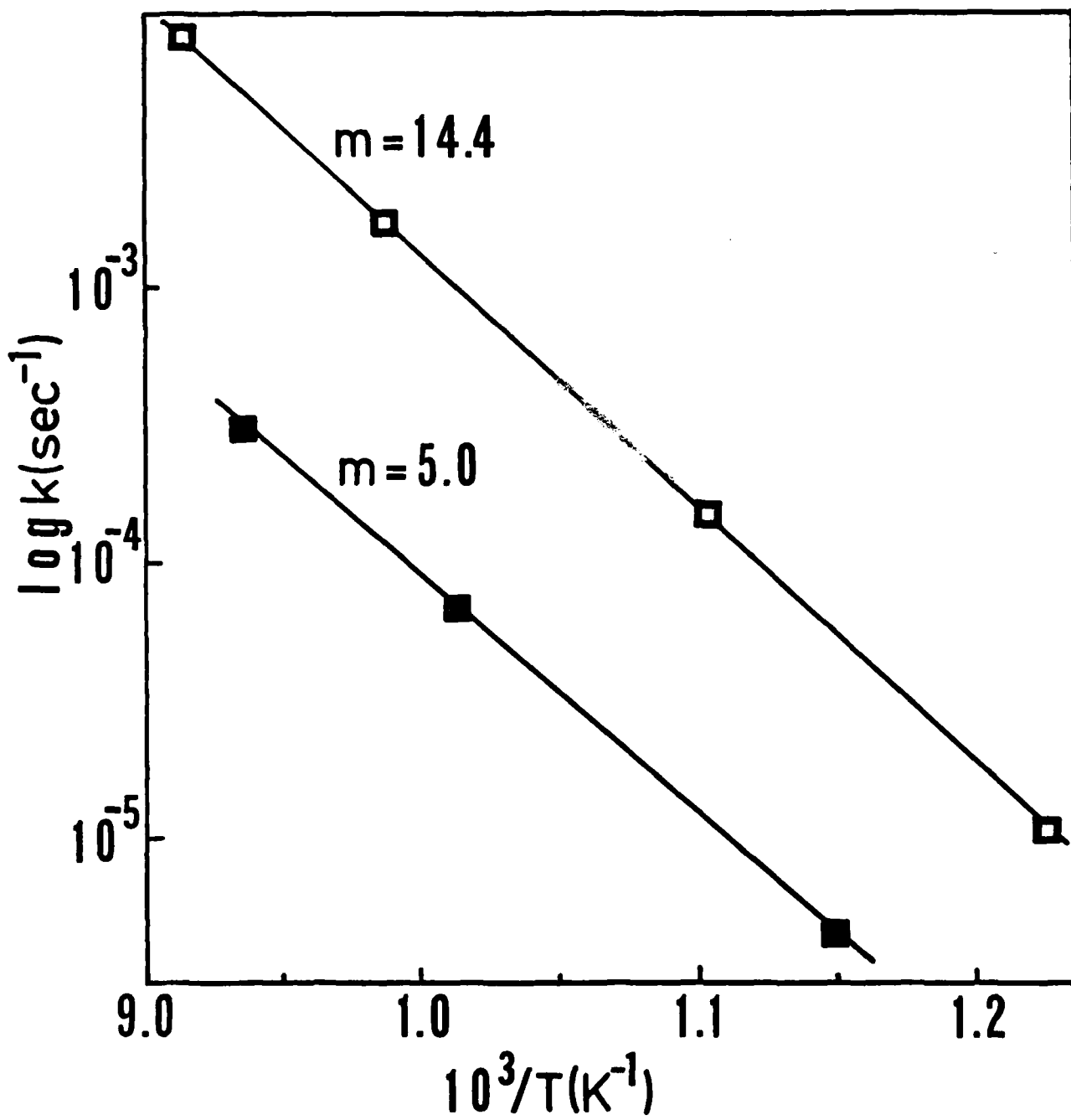


Fig. 2. Huan et al.

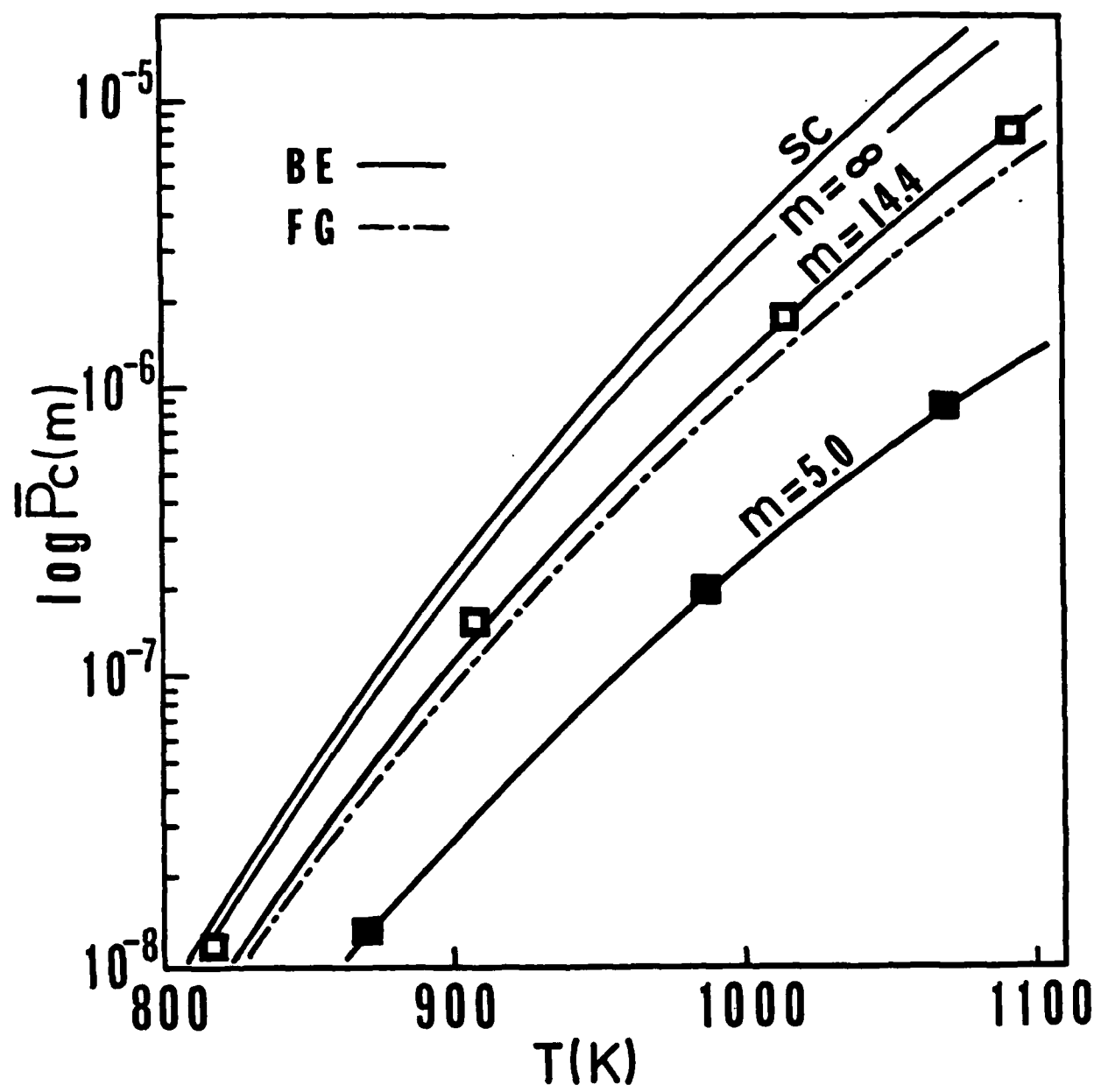


Fig. 3 Yuan et al.

INIT

DISTRIBUTION LIST

January 15, 1982

<u>No. Copies</u>		<u>No. Copies</u>
Dr. L.V. Schmidt Assistant Secretary of the Navy (R,E, and S) Room 5E 731 Pentagon Washington, D.C. 20350	1	Dr. F. Roberto Code AFRPL MKPA Edwards AFB, CA 93523
Dr. A.L. Slafkosky Scientific Advisor Commandant of the Marine Corps Code RD-1 Washington, D.C. 20380		Dr. L.H. Caveny Air Force Office of Scientific Research Directorate of Aerospace Sciences Bolling Air Force Base Washington, D.C. 20332
Dr. Richard S. Miller Office of Naval Research Code 413 Arlington, VA 22217	10	Mr. Donald L. Ball Air Force Office of Scientific Research Directorate of Chemical Sciences Bolling Air Force Base Washington, D.C. 20332
Mr. David Siegel Office of Naval Research Code 260 Arlington, VA 22217	1	Dr. John S. Wilkes, Jr. FJSRL/NC USAF Academy, CO 80840
Dr. R.J. Marcus Office of Naval Research Western Office 1030 East Green Street Pasadena, CA 91106	1	Dr. R.L. Lou Aerojet Strategic Propulsion Co. P.O. Box 15699C Sacramento, CA 95813
Dr. Larry Peebles Office of Naval Research East Central Regional Office 666 Summer Street, Bldg. 114-D Boston, MA 02210	1	Dr. V.J. Keenan Anal-Syn Lab Inc. P.O. Box 547 Paoli, PA 19301
Dr. Phillip A. Miller Office of Naval Research San Francisco Area Office One Hallidie Plaza, Suite 601 San Francisco, CA 94102	1	Dr. Philip Howe Army Ballistic Research Labs ARRADCOM Code DRDAR-BLT Aberdeen Proving Ground, MD 21005
Mr. Otto K. Heiney AFATL - DLDL Eglin AFB, FL 32542	1	Mr. L.A. Watermeier Army Ballistic Research Labs ARRADCOM Code DRDAR-BLI Aberdeen Proving Ground, MD 21005
Mr. R. Geisler ATTN: MKP/MS24 AFRPL Edwards AFB, CA 93523	1	Dr. W.W. Wharton Attn: DRSMI-RKL Commander U.S. Army Missile Command Redstone Arsenal, AL 35898

6/81

INIT

DISTRIBUTION LIST

<u>No. Copies</u>		<u>No. Copies</u>	
1	Mr. J. Murrin Naval Sea Systems Command Code 62R2 Washington, D.C. 20362	1	Dr. A. Nielsen Naval Weapons Center Code 385 China Lake, CA 93555
1	Dr. P.J. Pastine Naval Surface Weapons Center Code R04 White Oak Silver Spring, MD 20910	1	Dr. R. Reed, Jr. Naval Weapons Center Code 388 China Lake, CA 93555
1	Mr. L. Roslund Naval Surface Weapons Center Code R122 White Oak Silver Spring, MD 20910	1	Dr. L. Smith Naval Weapons Center Code 3205 China Lake, CA 93555
1	Mr. M. Stoss Naval Surface Weapons Center Code R121 White Oak Silver Spring, MD 20910	1	Dr. B. Douda Naval Weapons Support Center Code 5042 Crane, IN 47522
1	Dr. E. Zimmet Naval Surface Weapons Center Code R13 White Oak Silver Spring, MD 20910	1	Dr. A. Faulstich Chief of Naval Technology MAT Code 0716 Washington, D.C. 20360
1	Dr. D.R. Derr Naval Weapons Center Code 388 China Lake, CA 93555	1	LCDR J. Walker Chief of Naval Material Office of Naval Technology MAT, Code 0712 Washington, D.C. 20360
1	Mr. Lee N. Gilbert Naval Weapons Center Code 3205 China Lake, CA 93555	1	Mr. Joe McCartney Naval Ocean Systems Center San Diego, CA 92152
1	Dr. E. Martin Naval Weapons Center Code 3858 China Lake, CA 93555	1	Dr. S. Yamamoto Marine Sciences Division Naval Ocean Systems Center San Diego, CA 91232
1	Mr. R. McCarten Naval Weapons Center Code 3272 China Lake, CA 93555	1	Dr. G. Bosmajian Applied Chemistry Division Naval Ship Research & Development Center Annapolis, MD 21401
		1	Dr. H. Shuey Rohm and Haas Company Huntsville, AL 35801

6/81

INIT

DISTRIBUTION LIST

<u>No. Copies</u>		<u>No. Copies</u>	
Mr. R. Brown Naval Air Systems Command Code 330 Washington, D.C. 20361	1	Dr. J. Schnur Naval Research Lab. Code 6510 Washington, D.C. 20375	1
Dr. H. Rosenwasser Naval Air Systems Command AIR-310C Washington, D.C. 20360	1	Mr. R. Beauregard Naval Sea Systems Command SEA 64E Washington, D.C. 20362	1
Mr. B. Sobers Naval Air Systems Command Code 03P25 Washington, D.C. 20360	1	Mr. G. Edwards Naval Sea Systems Command Code 62R3 Washington, D.C. 20362	1
Dr. L.R. Rothstein Assistant Director Naval Explosives Dev. Engineering Dept. Naval Weapons Station Yorktown, VA 23691	1	Mr. John Boyle Materials Branch Naval Ship Engineering Center Philadelphia, PA 19112	1
Dr. Lionel Dickinson Naval Explosive Ordnance Disposal Tech. Center Code D Indian Head, MD 20640	1	Dr. H.G. Adolph Naval Surface Weapons Center Code R11 White Oak Silver Spring, MD 20910	1
Mr. C.L. Adams Naval Ordnance Station Code PM4 Indian Head, MD 20640	1	Dr. T.D. Austin Naval Surface Weapons Center Code R16 Indian Head, MD 20640	1
Mr. S. Mitchell Naval Ordnance Station Code 5253 Indian Head, MD 20640	1	Dr. T. Hall Code R-11 Naval Surface Weapons Center White Oak Laboratory Silver Spring, MD 20910	1
Dr. William Tolles Dean of Research Naval Postgraduate School Monterey, CA 93940	1	Mr. G.L. Mackenzie Naval Surface Weapons Center Code R101 Indian Head, MD 20640	1
Naval Research Lab. Code 6100 Washington, D.C. 20375	1	Dr. K.F. Mueller Naval Surface Weapons Center Code R11 White Oak Silver Spring, MD 20910	1

INIT

4

6/81

DISTRIBUTION LIST

	<u>No. Copies</u>		<u>No. Copies</u>
Dr. R.G. Rhoades Commander Army Missile Command DRSMI-R Redstone Arsenal, AL 35898	1	Dr. E.H. Debutts Hercules Inc. Baccus Works P.O. Box 98 Magna, UT 84044	1
Dr. W.D. Stephens Atlantic Research Corp. Pine Ridge Plant 7511 Wellington Rd. Gainesville, VA 22065	1	Dr. James H. Thacher Hercules Inc. Magna Baccus Works P.O. Box 98 Magna, UT 84044	1
Dr. A.W. Barrows Ballistic Research Laboratory USA ARRADCOM DRDAR-BLP Aberdeen Proving Ground, MD 21005	1	Mr. Theodore M. Gilliland Johns Hopkins University APL Chemical Propulsion Info. Agency Johns Hopkins Road Laurel, MD 20810	1
Dr. C.M. Frey Chemical Systems Division P.O. Box 358 Sunnyvale, CA 94086	1	Dr. R. McGuire Lawrence Livermore Laboratory University of California Code L-324 Livermore, CA 94550	1
Professor F. Rodriguez Cornell University School of Chemical Engineering Olin Hall Ithaca, NY 14853	1	Dr. Jack Linsk Lockheed Missiles & Space Co. P.O. Box 504 Code Org. 83-10, Bldg. 154 Sunnyvale, CA 94088	1
Defense Technical Information Center DTIC-DDA-2 Cameron Station Alexandria, VA 22314	12	Dr. B.G. Craig Los Alamos National Lab P.O. Box 1663 NSP/DOD, MS-245 Los Alamos, NM 87545	1
Dr. Rocco C. Musso Hercules Aerospace Division Hercules Incorporated Alleghany Ballistic Lab P.O. Box 210 Washington, DC 21502	1	Dr. R.L. Rabie WX-2, MS-952 Los Alamos National Lab. P.O. Box 1663 Los Alamos, NM 87545	1
Dr. Ronald L. Simmons Hercules Inc. Eglin AFATL/DLDL Eglin AFB, FL 32542	1	Dr. R. Rogers Los Alamos Scientific Lab. WX-2 P.O. Box 1663 Los Alamos, NM 87545	1

6/81

DISTRIBUTION LIST

<u>No. Copies</u>		<u>No. Copies</u>	
Dr. J.F. Kincaid Strategic Systems Project Office Department of the Navy Room 901 Washington, D.C. 20376	1	Dr. C.W. Vriesen Thiokol Elkton Division P.O. Box 241 Elkton, MD 21921	1
Strategic Systems Project Office Propulsion Unit Code SP2731 Department of the Navy Washington, D.C. 20376	1	Dr. J.C. Hinshaw Thiokol Wasatch Division P.O. Box 524 Brigham City, UT 83402	1
Mr. E.L. Throckmorton Strategic Systems Project Office Department of the Navy Room 1048 Washington, D.C. 20376	1	U.S. Army Research Office Chemical & Biological Sciences Division P.O. Box 12211 Research Triangle Park, NC 27709	1
Dr. D.A. Flanigan Thiokol Huntsville Division Huntsville, AL 35807	1	Dr. R.F. Walker USA ARRADCOM DRDAR-LCE Dover, NJ 07801	1
Mr. G.F. Mangum Thiokol Corporation Huntsville Division Huntsville, AL 35807	1	Dr. T. Sinden Munitions Directorate Propellants and Explosives Defense Equipment Staff British Embassy 3100 Massachusetts Ave. Washington, D.C. 20008	1
Mr. E.S. Sutton Thiokol Corporation Elkton Division P.O. Box 241 Elkton, MD 21921	1	Mr. J.M. Frankle Army Ballistic Research Labs ARRADCOM Code DRDAR-BLI Aberdeen Proving Ground, MD 21005	1
Dr. G. Thompson Thiokol Wasatch Division MS 240 P.O. Box 524 Brigham City, UT 84302	1	Dr. Ingo W. May Army Ballistic Research Lab ARRADCOM Code DRDAR-BLI Aberdeen Proving Ground, MD 21005	1
Dr. T.F. Davidson Technical Director Thiokol Corporation Government Systems Group P.O. Box 9258 Ogden, UT 84409	1		

INIT

6/81

DISTRIBUTION LISTNo. Copies

E. J. Palm Commander Army Missile Command DRSMI-RK Redstone Arsenal, AL 35898	1	Dr. Kenneth O Hartman Hercules Aerospace Division Hercules Incorporated Allegany Ballistics Lab P.O. Box 210 Cumberland, MD 21502	1
Dr. Merrill K. King Atlantic Research Corp. 5390 Cherokee Avenue Alexandria, VA 22314	1	Dr. Joyce J. Kaufman The Johns Hopkins University Department of Chemistry Baltimore, MD 21218	1
Dr. R.J. Bartlett Batelle Columbus Laboratories 505 King Avenue Columbus, OH 43201	1	Dr. John K. Dienes T-3, MS-216 Los Alamos National Lab P.O. Box 1663 Los Alamos, NM 87544	1
Dr. P. Rentzepis Bell Laboratories Murray Hill, NJ 07971	1	Dr. H.P. Marshall Dept. 52-35, Bldg. 204.2 Lockheed Missile & Space Co. 3251 Hanover Street Palo Alto, CA 94304	1
Professor Y.T. Lee Department of Chemistry University of California Berkeley, CA 94720	1	Professor John Deutsch MIT Department of Chemistry Cambridge, MA 02139	1
Professor M. Nicol Department of Chemistry 405 Hilgard Avenue University of California Los Angeles, CA 90024	1	Professor Barry Kunz College of Sciences & Arts Department of Physics Michigan Technological Univ. Houghton, MI 49931	1
Professor S.S. Penner University of California Energy Center Mail Code B-010 La Jolla, CA 92093	1	Dr. R. Bernecker Code R13 Naval Surface Weapons Center White Oak Silver Spring, MD 20910	1
Professor Curt Wittig University of Southern CA Dept. of Electrical Engineering University Park Los Angeles, CA 90007	1	Dr. C.S. Coffey Naval Surface Weapons Center Code R13 White Oak Silver Spring, MD 20910	1

INIT

6/81

DISTRIBUTION LISTNo. Copies

Dr. W. L. Elban Code R13 Naval Surface Weapons Center White Oak Silver Spring, MD 20910	1
Mr. K.J. Graham Naval Weapons Center Code 3835 China Lake, CA 93555	1
Dr. B. Junker Office of Naval Research Code 421 Arlington, VA 22217	1
Prof. H.A. Rabitz Department of Chemistry Princeton University Princeton, NH 08540	1
Dr. M. Farber Space Sciences, Inc. 135 West Maple Avenue Monrovia, CA 91016	1
Mr. M. Hill SRI International 333 Ravenswood Avenue Menlo Park, CA 94025	1
U.S. Army Research Office Engineering Division Box 12211 Research Triangle Park, NC 27709	1
U.S. Army Research Office Metallurgy & Materials Sci. Div. Box 12211 Research Triangle Park, NC 27709	1
Professor G.D. Duvall Washington State University Department of Physics Pullman, WA 99163	1

END
DATE
FILMED
3-82
DTIC